

Large-scale bias in the Universe: bispectrum method

S. Matarrese¹, L. Verde^{1,2}, A.F. Heavens²

¹ *Dipartimento di Fisica Galileo Galilei, Università di Padova, via Marzolo 8, I-35131 Padova, Italy*

² *Institute for Astronomy, University of Edinburgh, Royal Observatory, Blackford Hill, Edinburgh EH9 3HJ, United Kingdom*

14 August 2018

ABSTRACT

Evidence that the Universe may be close to the critical density, required for its expansion eventually to be halted, comes principally from dynamical studies of large-scale structure. These studies either use the observed peculiar velocity field of galaxies directly, or indirectly by quantifying its anisotropic effect on galaxy clustering in redshift surveys. A potential difficulty with both such approaches is that the density parameter Ω_0 is obtained only in the combination $\beta = \Omega_0^{0.6}/b$, if linear perturbation theory is used. The determination of the density parameter Ω_0 is therefore compromised by the lack of a good measurement of the bias parameter b , which relates the clustering of sample galaxies to the clustering of mass.

In this paper, we develop an idea of Fry (1994), using second-order perturbation theory to investigate how to measure the bias parameter on large scales. The use of higher-order statistics allows the degeneracy between b and Ω_0 to be lifted, and an unambiguous determination of Ω_0 then becomes possible. We apply a likelihood approach to the bispectrum, the three-point function in Fourier space. This paper is the first step in turning the idea into a practical proposition for redshift surveys, and is principally concerned with noise properties of the bispectrum, which are non-trivial. The calculation of the required bispectrum covariances involves the six-point function, including many noise terms, for which we have developed a generating functional approach which will be of value in calculating high-order statistics in general.

Key words: galaxies: bias - galaxies: clustering - large-scale structure of Universe

1 INTRODUCTION

The assumption that bright galaxies are *biased* tracers of the mass distribution has featured strongly in theories of galaxy and structure formation in recent years. The idea that galaxies are biased even on large scale has been studied for example by Peacock & Heavens (1985) and Bardeen et al. (1986), where galaxies are hypothesized as forming at high peaks of the density field filtered on relatively small scales. The concept of bias was then further extended to the extreme case where galaxies are painted on arbitrarily on the mass distribution. However, some constraints can be imposed, when the galaxy density is an arbitrary local function of the mass density. In this case, the bias (here defined in terms of the two-point correlation function) must be a monotonic function of the spatial separation (Coles 1993) if it derives from a Gaussian field. Numerical experiments show that this also holds for the power spectrum (Mann, Peacock & Heavens 1997).

It has been suggested that the bias mechanism can be modulated by environment dependent effects, as for example in the Cooperative Galaxy Formation model (Bower et

al. 1993). The net result of this modification of the standard scheme is that the relationship between the density fluctuation field $\delta(\vec{x})$ and the galaxy fluctuation field $\delta_g(\vec{x})$ becomes non-local and the bias turns out to be scale-dependent. Other bias possibilities include dynamical friction effects, allowing galaxies to settle in clusters (Couchman & Carlberg 1992). Note that even if the physical mechanism responsible for the bias operates only on relatively small scales, (e.g. within cluster cores), the bias parameter may differ from unity on much larger scales (Mann, Peacock & Heavens 1997), with long wavelength modes having to have enhanced amplitude to fit the higher peaks of density in clusters. If the bias arises physically in the epoch of galaxy formation, it will evolve in time, and will approach unity if galaxy numbers are preserved (Fry 1996, Nusser & Davis 1994). This condition may be broken by mergers (e.g. Matarrese et al. 1997), but also by luminosity evolution, if the sample is defined by a flux criterion, so it is safest to make no assumptions about bias evolution.

There are clearly many ideas, but we have really very little idea of how bias works and evolves in practice, and there is therefore strong motivation to find ways to measure

arXiv:astro-ph/9706059v2 16 Jun 1997

it empirically from the galaxy distribution. The main motivation, however, comes from the desire to split the degeneracy between Ω_0 and b which arises in linear perturbation theory from dynamical studies of large-scale structure. Both direct studies of the peculiar velocity field (e.g. Dekel et al. 1993) and studies of the distortion which peculiar velocities give to redshift-space galaxy maps (Kaiser 1987, Hamilton 1992, Fisher, Scharf & Lahav 1994, Heavens & Taylor 1995, Ballinger, Heavens & Taylor 1995) yield a value of

$$\beta \equiv \frac{\Omega_0^{0.6}}{b},$$

but not Ω_0 or b separately. The ignorance of the bias parameter compromises all conclusions about the real prize – Ω_0 , from large-scale structure studies.

With good data, probably available in the next few years from the new generation of galaxy surveys, we show that the bias parameter can be measured by studying higher-order characteristics of the density field. More specifically this is done by analyzing the bispectrum: the Fourier transform of the three-point correlation function (e.g. Frieman & Gaztañaga 1994). This statistic has the advantage that the determinations of the bispectrum can be made uncorrelated on different scales, or if not, their correlation properties can be calculated, and the choice of modes to analyse can be made to maximize signal-to-noise. These allow the bias parameter to be estimated via likelihood methods, importantly allowing error bars to be placed on the parameter estimates. The higher-order statistics work by exploiting the fact that gravitational instability skews the density field to high densities as it evolves. This behaviour can also be mimicked by non-linear biasing, but these two effects can be separated by the use of shape information: essentially non-linear biasing of a truly Gaussian field will lead to different shaped structures from a non-Gaussian field arising from gravitational instability.

It is worth making a few remarks about the advantages of performing this sort of analysis in Fourier space rather than via high-order correlation functions in real space. The main advantage, which is shared by the power spectrum, is that the estimates of the correlation functions in Fourier space can be made uncorrelated (or at least their correlation properties can be readily calculated), with enormous benefits for estimation of parameters and error bars. The second advantage is that the real-space determinations of high-order correlations are really only known well in the non-linear regime, where perturbation theory may not apply. In Fourier space, there is a clear separation of scales where perturbation theory works and breaks down.

Translating this idea into a practical algorithm requires a number of issues to be tackled, including the effects of a varying selection function and redshift distortions, and the non-trivial issue of what shot noise terms appear in the required six-point function. This paper is principally concerned with the error analysis; a subsequent paper will present a study of the other issues.

The plan of this paper is as follows. In Section 2 we introduce the second-order perturbation expansion for the (unknown) matter density field and the (observable) galaxy density field. The necessary mathematical techniques to calculate the N -point functions, including shot noise, are given in Section 3. Sections 4 discusses optimal methods and prac-

tical implementation to a numerical simulation of the galaxy distribution, and Section 5 discusses the results and the possibilities of practical application to real data.

2 SECOND ORDER APPROXIMATION

As Fry (1994) pointed out, since the degeneracy between Ω_0 and b is an intrinsic feature of the linear theory, one needs to go to second order in order to separate the parameters.

Under the assumption that the initial fluctuation are Gaussian and that structure grows by gravitational instability, the three-point correlation function is intrinsically a second-order quantity, and should be detectable in the mildly non-linear regime where second-order perturbation theory is a reliable description.

The data we will use to constrain the bias parameter will be the real part of the three-point function in k -space:

$$D_\alpha = \text{Re}(\delta_{\vec{k}_1} \delta_{\vec{k}_2} \delta_{\vec{k}_3}), \quad (1)$$

for closed triangles. α is shorthand for the triangle specified by some triplet of k -vectors. $\delta_{\vec{k}} \equiv \int d^3\vec{r} \delta(\vec{r}) \exp(-i\vec{k} \cdot \vec{r})$ is the Fourier transform of the fractional overdensity field $\delta(\vec{x}) \equiv n(\vec{x})/\bar{n} - 1$, where n is the number density of galaxies, and \bar{n} its mean. D_α is related to the bispectrum $B(\vec{k}_1, \vec{k}_2, \vec{k}_3)$ by

$$\langle \delta_{\vec{k}_1} \delta_{\vec{k}_2} \delta_{\vec{k}_3} \rangle = (2\pi)^3 B(\vec{k}_1, \vec{k}_2, \vec{k}_3) \delta^D(\vec{k}_1 + \vec{k}_2 + \vec{k}_3) = \langle D_\alpha \rangle, \quad (2)$$

where $\delta^D(\vec{k})$ is the three-dimensional Dirac delta function and the $\langle \rangle$ indicates ensemble average, or, by the ergodic theorem, the average over a large volume. In what follows, we may occasionally refer loosely to D_α as the bispectrum.

We expand the density field to second order as:

$$\delta(\vec{x}) = \delta^{(1)}(\vec{x}) + \delta^{(2)}(\vec{x}), \quad (3)$$

where $\delta^{(2)}$ is $O(\delta^{(1)2})$ and represents departures from Gaussian behaviour.

Note that what we are dealing here is not a mildly non-linear field, but a highly nonlinear field which is filtered on some smoothing scale. The operations of smoothing and gravitational evolution do not commute, so there is some possibility that perturbation theory might be inaccurate. However, this problem is not unique to second-order perturbation theory: it exists in even for the evolution of the power spectrum, which for practical cases can be treated well by perturbation theory. Experiments on the bispectrum by others and ourselves (see section 4) show that perturbation theory for the implicitly filtered fields works well if the smoothed field is not too nonlinear.

2.1 Unbiased case

For an unbiased distribution (or for the matter distribution) we can expand $\langle \delta_1 \delta_2 \delta_3 \rangle$ to second order, obtaining:

$$\begin{aligned} \langle \delta_1 \delta_2 \delta_3 \rangle &\simeq \langle \delta_1^{(1)} \delta_2^{(1)} \delta_3^{(1)} \rangle \\ &+ \langle \delta_1^{(1)} \delta_2^{(1)} \delta_3^{(2)} \rangle + \text{cyclic terms}(231, 312). \end{aligned} \quad (4)$$

Only the second term of this survives. Since we will work in Fourier space we quote directly the expression for $\delta_{\vec{k}}^{(2)}$, the Fourier transform of $\delta^{(2)}(\vec{x})$ (Catelan et al. 1995):

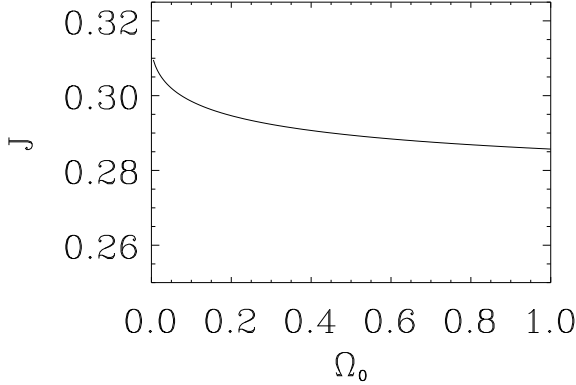


Figure 1. The weak dependence of J on Ω_0 for equilateral triangles.

$$\delta_{\vec{k}}^{(2)} = \frac{1}{(2\pi)^3} \int d^3k_a d^3k_b \delta^D(\vec{k}_a + \vec{k}_b - \vec{k}) J(\vec{k}_a, \vec{k}_b) \delta_{\vec{k}_a}^{(1)} \delta_{\vec{k}_b}^{(1)}, \quad (5)$$

where

$$J(\vec{k}_1, \vec{k}_2, \Omega_0) = 1 - B(\Omega_0) + \frac{\vec{k}_1 \cdot \vec{k}_2}{2k_1 k_2} \left(\frac{k_1}{k_2} + \frac{k_2}{k_1} \right) + B(\Omega_0) \left(\frac{\vec{k}_1 \cdot \vec{k}_2}{k_1 k_2} \right)^2. \quad (6)$$

B is a function which is $2/7$ for an Einstein-de Sitter universe, in which case the expression above reduces to the form originally obtained by Goroff et al. (1986). The useful feature of this is that J is almost independent of Ω_0 , as seen in Fig. 1, so we can use the Einstein-de Sitter value with minimal error.

The bispectrum for the unbiased case, in the absence of shot noise, is therefore

$$\langle \delta_{\vec{k}_1} \delta_{\vec{k}_2} \delta_{\vec{k}_3} \rangle = (2\pi)^3 [2J(\vec{k}_1, \vec{k}_2) P(k_1) P(k_2) + cyc.] \times \delta^D(\vec{k}_1 + \vec{k}_2 + \vec{k}_3), \quad (7)$$

where the linear power spectrum is defined in terms of the orthogonality of the transform coefficients, arising from homogeneity:

$$\langle \delta_{\vec{k}_1} \delta_{\vec{k}_2} \rangle = (2\pi)^3 P(k) \delta^D(\vec{k}_1 + \vec{k}_2). \quad (8)$$

For practical cases, the transform is made in a finite box, when the Dirac delta function is modified (see Section 3.3).

2.2 Biased case

We assume that the biased (galaxy) density is a local function of the unbiased (matter) density. Galaxy properties will be identified by the subscript g ; matter fields have no subscript. We make a Taylor expansion of the galaxy density to second order in $\delta^{(1)}$, so for consistency we must include an extra quadratic bias term b_2 :

$$\delta_g(\vec{x}) = f[\delta(\vec{x})]$$

$$\begin{aligned} &\simeq b_1 \delta(\vec{x}) + \frac{1}{2} b_2 \delta^2(\vec{x}) \\ &\simeq b_1 \delta^{(1)}(\vec{x}) + b_1 \delta^{(2)}(\vec{x}) + \frac{1}{2} b_2 \delta^{(1)2}(\vec{x}). \end{aligned} \quad (9)$$

The linear bias parameter b_1 is to be identified with b . Notice that the expression above is not correctly normalised: a term $b_2 \langle \delta^{(1)2} \rangle / 2$ needs to be subtracted so that the biased field has zero mean. As we will be working in Fourier space, this extra term is irrelevant for all except the $\vec{k} = \vec{0}$ mode, and will be ignored*.

Following the same procedure as in the unbiased case we obtain to second order

$$\begin{aligned} \langle \delta_{g1} \delta_{g2} \delta_{g3} \rangle &= b_1^3 \langle \delta_1^{(1)} \delta_2^{(1)} \delta_3^{(1)} \rangle \\ &+ b_1^3 \langle \delta_1^{(1)} \delta_2^{(1)} \delta_3^{(2)} \rangle + cyc. \\ &+ \frac{b_1^2 b_2}{2} \langle \delta_1^{(1)} \delta_2^{(1)} \delta_3^{(1)2} \rangle + cyc. \end{aligned} \quad (10)$$

Once again, the first term vanishes. We can re-write the last term by exploiting the cumulant expansion theorem for the four-point function obtaining the non-vanishing terms

$$\langle \delta_1^{(1)} \delta_2^{(1)} \rangle \langle \delta_3^{(1)2} \rangle + 2 \langle \delta_1^{(1)} \delta_3^{(1)} \rangle \langle \delta_2^{(1)} \delta_3^{(1)} \rangle. \quad (11)$$

Therefore to second order the galaxy bispectrum is:

$$\begin{aligned} \langle \delta_{g\vec{k}_1} \delta_{g\vec{k}_2} \delta_{g\vec{k}_3} \rangle &= \\ (2\pi)^3 \{ &b_1^3 [P(\vec{k}_1) P(\vec{k}_2) 2J(\vec{k}_1, \vec{k}_2) + cyc.] \\ &+ b_1^2 b_2 [P(\vec{k}_1) P(\vec{k}_2) + cyc.] \} \delta^D(\vec{k}_1 + \vec{k}_2 + \vec{k}_3). \end{aligned} \quad (12)$$

From this we see how the bispectrum may be used to estimate the bias parameters. J is almost independent of Ω_0 , so a set of triangles in k -space can in principle allow us to measure the bias parameters b_1 and b_2 . It is important to realise that it is necessary to consider triangles of different shapes to lift a new degeneracy between b_1 and b_2 , since triangles of a common shape have the same J and (12) then gives information only on the combination $b_1^2(2b_1J + b_2)$. The same sort of degeneracy has been noted for the 3-point function in real space (see Frieman & Gaztañaga 1994). The strong dependence on shape has been illustrated (e.g. Jing, Börner & Valdarnini 1995), but there appears to be little work on using different shapes to lift the degeneracy. We return to the physical reasons for having to take more than one shape in the discussion.

We wish to estimate b_1 and b_2 by maximum likelihood, so we need an estimate of the shot noise, and the covariance between bispectrum estimates. We turn to this in the next section, but here note that the bispectrum (strictly defined in terms of the mean) is a real quantity. This is a result of isotropy - the bispectrum does not depend on which direction round the triangle is taken. Accordingly we use only

* It is not obvious that a physical mechanism will lead to a functional dependence which can be expanded in a Taylor series. Examples are the ‘weighted bias’ model studied by Catelan et al. (1994) and the ‘censoring bias’ studied by Mann, Peacock & Heavens (1997). It is an open question whether such schemes might be approximated by a continuous $\delta_g(\delta)$ relation when smoothed on larger scales.

the real parts of $\delta_{g\vec{k}_1} \delta_{g\vec{k}_2} \delta_{g\vec{k}_3}$, as our data, as the imaginary parts just introduce more noise.

Since $P(\vec{k})$ is unknown, we write (12) in terms of potentially observable quantities, the linear galaxy power spectrum $P_g = b_1^2 P$ (equal to the observed power spectrum at adequate order for second-order perturbation theory):

$$\begin{aligned} & \langle \delta_{g\vec{k}_1} \delta_{g\vec{k}_2} \delta_{g\vec{k}_3} \rangle = \\ & (2\pi)^3 \left\{ c_1 \left[2P_g(\vec{k}_1)P_g(\vec{k}_2)J(\vec{k}_1, \vec{k}_2) + cyc. \right] \right. \\ & \left. + c_2 \left[P_g(\vec{k}_1)P_g(\vec{k}_2) + cyc. \right] \right\} \delta^D(\vec{k}_1 + \vec{k}_2 + \vec{k}_3), \end{aligned} \quad (13)$$

where

$$c_1 \equiv \frac{1}{b_1}; \quad c_2 \equiv \frac{b_2}{b_1^2}. \quad (14)$$

Under the assumption of a uniform prior for the quantities c_1 & c_2 , the *a posteriori* probability for the parameters is the likelihood:

$$\begin{aligned} \mathcal{L}(c_1, c_2) &= \frac{1}{(2\pi)^{\frac{M}{2}} (\det C)^{\frac{1}{2}}} \\ & \exp \left[-\frac{1}{2} \sum_{\alpha\beta} (D_\alpha - \mu_\alpha) C_{\alpha\beta}^{-1} (D_\beta - \mu_\beta) \right], \end{aligned} \quad (15)$$

where the means of the M data are $\mu_\alpha(b_1, b_2) \equiv \langle D_\alpha \rangle$ and $C_{\alpha\beta} \equiv \langle (D_\alpha - \mu_\alpha)(D_\beta - \mu_\beta) \rangle$ is the covariance matrix, which is also a function of the bias parameters. The use of a Gaussian likelihood function is justified if there are many contributing data, whether or not they themselves have Gaussian distributions, provided the sensitivity to the parameters is through the mean rather than the variance. It is straightforward to show that, by using the mean of many observed data drawn from the same distribution, the likelihood is identical (by the Central Limit Theorem) as the Gaussian likelihood for the individual data, with the same variance and mean. In our case the variance is only weakly dependent on the parameters, through the shot noise, so our use of a Gaussian likelihood function is quite justified.

Note that our data are real $D_\alpha = Re(Z_\alpha) \equiv Re(\delta_{\vec{k}_1} \delta_{\vec{k}_2} \delta_{\vec{k}_3})$, and we can write the covariance matrix for D_α in terms of the complex Z_α :

$$\langle D_\alpha D_\beta \rangle = \frac{1}{2} Re \left[\langle Z_\alpha Z_\beta \rangle + \langle Z_\alpha Z_\beta^* \rangle \right]. \quad (16)$$

It should be obvious that we require the six-point function to calculate the covariance matrix, and we also need to include shot noise in the bispectrum estimates. The former is sufficiently complicated by the presence of a very large number of noise terms that we present a general method for doing calculations of this nature in the next section.

3 STATISTICS OF RANDOM FIELDS AND DERIVATION OF THE PENTASPECTRUM

This section presents a mathematical method for calculating N -point distributions in Fourier space for continuous and discrete fields, and deal also with the realistic case of a galaxy survey with a non-uniform number density (arising,

for example, from a flux-limited catalogue). These distributions are required to calculate the covariance properties of the bispectrum. A reader interested principally in the application of the bispectrum may omit this at a first sitting.

The complete description of a random field is given by the *probability distribution functional* \mathcal{P} , which should be thought as the continuous limit of the joint probability distribution in N points, as $N \rightarrow \infty$. To describe the statistics of a general random field $f(\vec{x})$, we need to know the functional $\mathcal{P}[f(\vec{x})]$, which specifies the distribution of the possible values of f at each point. By statistical homogeneity $\mathcal{P}[f(\vec{x})]$ will be independent of \vec{x} . Consider then the *partition functional* or *generating functional of the correlation functions* \mathcal{Z} defined as a functional integral, as follows:

$$\begin{aligned} \mathcal{Z}[\mathcal{J}(x)] &\equiv \int \mathcal{D}[f] \mathcal{P}[f] \exp \left(i \int d^3x \mathcal{J}(\vec{x}) f(\vec{x}) \right) \\ &= \left\langle \exp \left[i \int d^3x \mathcal{J}(\vec{x}) f(\vec{x}) \right] \right\rangle, \end{aligned} \quad (17)$$

where $\mathcal{J}(\vec{x})$ is an external source perturbing the underlying statistics and $\mathcal{D}[f]$ is a suitable measure such that the probability distribution is correctly normalized to 1: $\int \mathcal{D}[f(\vec{x})] \mathcal{P}[f(\vec{x})] = 1$.

From this function we can recover the *correlation functions* μ_N of the distribution and the *connected correlation functions* or κ_N as follows:

- From the *generating functional of the correlation functions*

$$\mu_N \equiv \langle f(\vec{x}_1) \dots f(\vec{x}_N) \rangle = i^{-N} \frac{\delta^N \mathcal{Z}[\mathcal{J}]}{\delta \mathcal{J}(\vec{x}_1) \dots \delta \mathcal{J}(\vec{x}_N)}, \quad (18)$$

evaluated at $\mathcal{J} = 0$.

- From the *generating functional of the connected (or ‘reduced’) correlation functions*

$$\mathcal{K}[\mathcal{J}] \equiv \ln \mathcal{Z}[\mathcal{J}], \quad (19)$$

$$\begin{aligned} \kappa_N(\vec{x}_1 \dots \vec{x}_N) &= \langle f(\vec{x}_1) \dots f(\vec{x}_N) \rangle_{\text{connected}} \\ &= i^{-N} \frac{\delta^N \mathcal{K}[\mathcal{J}]}{\delta \mathcal{J}_1 \dots \delta \mathcal{J}_N}, \end{aligned} \quad (20)$$

evaluated at $\mathcal{J} = 0$.

From the above definitions it follows that a complete characterization of the statistics, i.e. the complete knowledge of the partition functional, requires the knowledge of the correlation functions of all orders. In fact it is usually possible to recover the partition functional as

$$\begin{aligned} \mathcal{Z}[\mathcal{J}] &= 1 + \sum_{n=1}^{\infty} \frac{i^n}{n!} \int d\vec{x}_1 \dots d\vec{x}_n \mu_n(\vec{x}_1, \dots, \vec{x}_n) \times \\ & \mathcal{J}(\vec{x}_1) \dots \mathcal{J}(\vec{x}_n) \end{aligned} \quad (21)$$

and similarly for $\mathcal{K}[\mathcal{J}]$ in terms of the connected correlation functions,

$$\begin{aligned} \mathcal{K}[\mathcal{J}] &= \sum_{n=1}^{\infty} \frac{i^n}{n!} \int d\vec{x}_1 \dots d\vec{x}_n \kappa_n(\vec{x}_1, \dots, \vec{x}_n) \times \\ & \mathcal{J}(\vec{x}_1) \dots \mathcal{J}(\vec{x}_n). \end{aligned} \quad (22)$$

The expansion of correlation functions of order N in terms of connected correlation functions of order $M \leq N$, i.e. the Cumulant (or Cluster) Expansion (e.g. Kendall & Stewart 1977, van Kampen 1992), follows trivially from equations (21) and (22). The cluster expansion is widely used in statistical mechanics where it constitutes the basis for approximation schemes in studying slightly non-ideal many-body systems like gases or fluids (Rice & Gray 1965). A review of the use of functional integration in cosmology can be found e.g. in Fry (1984), Bertschinger (1992), Matsubara (1995). It is worthwhile, at this point, to make some remarks on applicability. In dealing with slightly imperfect fluids it is assumed that the interaction falls off faster than $\frac{1}{r^3}$, this allows one to neglect the connected higher-order terms; in the case of gravity we must be aware that this is not generally true. The connected correlation functions κ_N , which are closely related to the connected Green's functions of quantum field theory (e.g. Ramond 1989), are defined by the above procedure in such a way that any separable contribution of the type $\langle f^M \rangle \langle f^{N-M} \rangle$ has been removed. As a consequence, if any subset of the N points is set to infinite separation the connected correlation function of order N goes to zero. These connected correlation functions of order N for the density fluctuation field are often simply called 'correlation functions' in the cosmological literature (e.g. Peebles 1980). An important property of these functions is that if the underlying statistics is Gaussian all the connected correlations of order higher than 2 vanish. Finally, when the covariance functions (and the connected analogous) are evaluated for $\vec{x}_1 = \vec{x}_2 = \dots = \vec{x}_N$, respectively the *moments* and the *cumulants* are obtained.

Continuous random fields and point processes (random distributions of discrete points) are both cases of random processes. It is possible to relate discrete and continuous distributions as we will see in the next paragraphs.

3.1 Discrete and continuous distributions

As already mentioned, the theory predicts the statistical properties of the continuous matter distribution, while observations are concerned with the galaxy distribution, which is discrete. Different biasing schemes have been introduced to relate the (theoretical) distribution of relative mass density fluctuations to the (observed) distribution of galaxies, but the true relation is still unknown. However, independently of the presence of bias, it is possible to relate formally one to the other.

In order to recover a continuous distribution from a discrete one, define for the discrete process the analogue of the density field, the number density field, as a sum over Dirac delta functions:

$$f(\vec{x}) = n(\vec{x}) = \bar{n}[1 + \delta(\vec{x})] \equiv \sum_i \delta^D(\vec{x} - \vec{x}_i),$$

$$\bar{n} = \left\langle \sum_i \delta^D(\vec{x} - \vec{x}_i) \right\rangle, \quad (23)$$

where \bar{n} is the mean number density.

Conversely, a simple way to generate a discrete distribution from a continuous one is to assume Poisson sampling (Peebles 1980, Bertschinger 1992, Fry 1985) by placing, at each volume element δV in the sample region, a point with

probability $\delta P = \rho(\vec{x})\delta V$, where $\rho(\vec{x})$ is the local mean density. The outcome is a double stochastic process, with one level of randomness coming from the random field and the second from the Poisson sampling[†]. It is then possible to take into account the effect of discreteness by performing a simple substitution in the partition functional or in the generating functional for the continuous case.

In the Poisson model if the probability of finding one object in an infinitesimal volume element δV at position \vec{x} is $P_1 = \rho(\vec{x})\delta V$, then the probability of finding no objects is $P_0 = 1 - \rho(\vec{x})\delta V$ and the probability of finding more than one object is an infinitesimal of higher order. To obtain the probability generating *functional* for the discrete process, we need to generalize this procedure to infinitely many small volumes. With this aim, we start from a given realization of the stochastic process and divide the volume in an infinite set of cells with individual volumes δV_ℓ . Then we consider the joint probability $P_{\{N_\ell\}}$ of finding N_1 objects in the volume δV_1 , N_2 in the volume δV_2 , etc.. and we define the generator of discrete counts in that realization as

$$\begin{aligned} \mathcal{Z}[\mathcal{J}] &= \sum_{\{N_\ell\}} P_{\{N_\ell\}} e^{i \sum_\ell N_\ell \mathcal{J}_\ell} \\ &= \prod_\ell [1 - \rho(\vec{x}_\ell)\delta V_\ell + \rho(\vec{x}_\ell)\delta V_\ell e^{i\mathcal{J}(\vec{x}_\ell)}] \\ &\cong \prod_\ell \exp[(e^{i\mathcal{J}(\vec{x}_\ell)} - 1)\rho(\vec{x}_\ell)\delta V_\ell]. \end{aligned} \quad (24)$$

We then let $\delta V_\ell \rightarrow 0$ in the given realization and average over the statistical ensemble of the underlying continuous field. This gives the required generating functional for the discretized process

$$\mathcal{Z}^d[\mathcal{J}] = \left\langle \exp \int d^3x [e^{i\mathcal{J}(\vec{x})} - 1] \rho(\vec{x}) \right\rangle. \quad (25)$$

Accounting for the effect of graininess therefore amounts to the substitution

$$i\mathcal{J} \rightarrow (e^{i\mathcal{J}} - 1) \quad (26)$$

in the generating functional for the continuous process. This result is a generalization of the standard procedure leading to the generating *function* for the moments of discrete counts in cells (e.g. Fry 1985). The practical utility of this method is that it permits calculation of correlated counts in different cells, according to the procedures described in Section 3.2 and Section 3.3 below.

Actually, there is a subtlety to point out here: the discrete process that we can observe is the one connected with the underlying continuous density distribution $\rho(\vec{x})$, but we want to study the statistics of the fractional over-density field $\delta = \rho(\vec{x})/\bar{\rho} - 1$ which has several advantages, mainly the fact that it has zero mean. To calculate its properties we have to modify slightly the above procedure. We first notice that the discrete version of the random field $1 + \delta$ is obtained by the substitution

[†] This procedure to account for discreteness is a model, and may not hold in practice. An example arises in Voronoi tessellations (see e.g. Williams, Peacock & Heavens 1991), where objects are placed at the intersections of Voronoi planes. This case can even result in sub-shot noise power.

$$i\mathcal{J} \rightarrow (e^{i\mathcal{J}/N} - 1)N, \quad (27)$$

where N is the average number of objects within the sampling volume, in the generating functional of $1 + \delta$. Next, to subtract the terms coming from the mean value 1, we use the fact that the generating functional for the sum of two independent random fields is just the product of the individual generating functionals. The discrete generating functional for δ is therefore

$$\mathcal{Z}[\mathcal{J}]_\delta = \exp \left\{ -i \int d^3x \mathcal{J}_{\text{cont}}(\vec{x}) \right\} \mathcal{Z}[\mathcal{J}]_{1+\delta} \quad (28)$$

because the generating functional for a uniform and continuous field of value 1 is simply $\exp \left[i \int d^3x \mathcal{J}_{\text{cont}}(\vec{x}) \right]$.

In the next section, we give explicit expressions for the source function \mathcal{J} , in real and Fourier space, and for continuous and discrete distributions.

3.2 N -point correlation functions in real and Fourier space

The quantity that we are dealing with is a complex number Z_α given by $\delta_{\vec{k}_1} \delta_{\vec{k}_2} \delta_{\vec{k}_3}$ where the vectors form a triangle: $\vec{k}_1 + \vec{k}_2 + \vec{k}_3 = \vec{0}$.

The average of Z_α over the ensemble (of closed triangles) is the bispectrum, but the actual quantity Z_α fluctuates across the ensemble. In order to quantify this fluctuation it would be valuable to estimate its covariance and this involves the quantity $\langle Z_\alpha Z_\beta \rangle$ (see equation 16).

This quantity is nothing but the six-point correlation function (not just the irreducible or connected one) in Fourier space (shot noise contribution included) in the particular case when the six vectors form two triangles:

$$\langle \delta_{\vec{k}_1} \delta_{\vec{k}_2} \dots \delta_{\vec{k}_6} \rangle, \quad (29)$$

where $\vec{k}_1 + \vec{k}_2 + \vec{k}_3 = \vec{0}$ and $\vec{k}_4 + \vec{k}_5 + \vec{k}_6 = \vec{0}$.

The formalism illustrated in section 3 has been introduced for this reason. Since we want to take into account the shot noise contribution, we need to work with the generating functional for the covariance functions of $1 + \delta(x)$ which is:

$$\begin{aligned} \mathcal{Z}[\mathcal{J}] &= \int \mathcal{D}(\delta) \mathcal{P}(\delta) \exp \left(i \int d^3x \mathcal{J}(\vec{x}) [1 + \delta(\vec{x})] \right) \\ &= \left\langle \exp \left\{ i \int d^3x \mathcal{J}(\vec{x}) [1 + \delta(\vec{x})] \right\} \right\rangle. \end{aligned} \quad (30)$$

Instead of dealing with functional derivation, we may write the ‘external source’ \mathcal{J} in a form which allows the functional derivatives to be replaced by normal differentiation (Matarrese, Lucchin & Bonometto 1986):

$$\mathcal{J}(\vec{x}) \equiv \sum_{m=1}^N s_m \delta^D(\vec{x} - \vec{x}_m). \quad (31)$$

The covariance functions up to the N^{th} order can then be obtained by the following differentiation:

$$\langle [1 + \delta(\vec{x}_1)] \dots [1 + \delta(\vec{x}_N)] \rangle = i^{-N} \left[\frac{\partial^N \mathcal{Z}[\mathcal{J}]}{\partial s_1 \dots \partial s_N} \right]_{s_m=0} \quad (32)$$

and the corresponding connected parts are obtained performing the same kind of differentiation on $\ln \mathcal{Z}[\mathcal{J}]$.

Smoothing can be incorporated easily. If the smoothed field is defined by the convolution:

$$\delta_{\text{smoothed}}(\vec{x}) \equiv \int d^3x' \delta(\vec{x}') W(\vec{x} - \vec{x}'), \quad (33)$$

the statistics of the smoothed field may be obtained by the substitution

$$\delta^D(\vec{x} - \vec{x}_m) \longrightarrow W(\vec{x} - \vec{x}_m) \quad (34)$$

in equation (31). For a discrete process the generating functional $\mathcal{Z}^d[\mathcal{J}]$ is obtained with the substitution (27).

In Fourier space, the N -point functions may be obtained by a straightforward change to the source function, which becomes the Fourier transform of the real-space \mathcal{J} . If $\widetilde{W}(\vec{k})$ is the transform of the smoothing function, then, for a continuous field,

$$\mathcal{J}_{\vec{k}}(\vec{x}) = \sum_{m=1}^N s_m e^{-i\vec{k} \cdot \vec{x}} \widetilde{W}(\vec{k}_m) \quad (35)$$

and in the discrete case:

$$\mathcal{J}_{\vec{k}}^d(\vec{x}) = -iN \left\{ \exp \left[\frac{i}{N} \sum_{m=1}^N s_m e^{-i\vec{k}_m \cdot \vec{x}} \widetilde{W}(\vec{k}_m) \right] - 1 \right\}. \quad (36)$$

In fact notice that the unsmoothed $\mathcal{J}_{\vec{k}}^d$ can be obtained from the \mathcal{J}^d just by substituting, in the exponential, the Dirac delta function by its Fourier transform.

Our *ansatz* for the generating functional is to assume that all correlations vanish above the 3-point function:

$$\begin{aligned} \mathcal{Z}[\mathcal{J}] &= \\ \exp \left[i \int d^3x \mathcal{J}(\vec{x}) - \frac{1}{2} \int d^3x d^3x' \mathcal{J}(\vec{x}) \mathcal{J}(\vec{x}') \xi_{\text{conn.}}^{(2)}(\vec{x}, \vec{x}') \right. \\ \left. - \frac{i}{6} \int d^3x d^3x' d^3x'' \mathcal{J}(\vec{x}) \mathcal{J}(\vec{x}') \mathcal{J}(\vec{x}'') \xi_{\text{conn.}}^{(3)}(\vec{x}, \vec{x}', \vec{x}'') \right]. \end{aligned} \quad (37)$$

The validity of this form relies on the fact that we are assuming Gaussian initial fluctuations. In the linear regime all the connected correlation function of order 3 or higher vanish. Allowing then for a quasi-linear evolution, and performing a second-order perturbation theory approximation, we allow $\xi^{(3)}$ to become non-zero, but we still rely on all the higher-order irreducible correlation functions being negligible.

Despite the conceptual simplicity of the algorithm introduced, it is quite cumbersome to perform the 6^{th} derivative of $\mathcal{Z}^d[\mathcal{J}]$, so for practical purposes we use the cluster expansion and express the six-point correlation function in terms of the connected parts of lower or equal orders.

$$\begin{aligned} \langle \delta_1 \dots \delta_6 \rangle^{d/c} &= \\ \langle \delta_1 \delta_2 \rangle_{\text{conn.}}^{d/c} \langle \delta_3 \delta_4 \rangle_{\text{conn.}}^{d/c} \langle \delta_5 \delta_6 \rangle_{\text{conn.}}^{d/c} &+ \dots 15 \text{ terms} \\ + \langle \delta_1 \delta_2 \rangle_{\text{conn.}}^{d/c} \langle \delta_3 \delta_4 \delta_5 \delta_6 \rangle_{\text{conn.}}^{d/c} &+ \dots 15 \text{ terms} \\ + \langle \delta_1 \delta_2 \delta_3 \rangle_{\text{conn.}}^{d/c} \langle \delta_4 \delta_5 \delta_6 \rangle_{\text{conn.}}^{d/c} &+ \dots 10 \text{ terms} \\ + \langle \delta_1 \dots \delta_6 \rangle_{\text{conn.}}^{d/c} & \end{aligned} \quad (38)$$

The d/c superscript stands for discrete or continuous case and it has been explicitly written to show that it is possible to treat the two cases, in configuration or Fourier space, on the same footing provided we make the corresponding substitution for the external source.

For our purposes the calculations have been made directly in Fourier space for the discrete case giving:

$$\langle \delta_i \delta_j \rangle_{\text{conn.}}^d = (2\pi)^3 \left[P(k_i) + \frac{1}{\bar{n}} \right] \delta^D(\vec{k}_i + \vec{k}_j), \quad (39)$$

$$\langle \delta_l \delta_m \delta_n \rangle_{\text{conn.}}^d = (2\pi)^3 \delta^D(\vec{k}_l + \vec{k}_m + \vec{k}_n) \times \left\{ B_{lmn} + \frac{1}{\bar{n}} [P(k_l) + P(k_m) + P(k_n)] + \frac{1}{\bar{n}^2} \right\}, \quad (40)$$

$$\langle \delta_o \delta_p \delta_q \delta_r \rangle_{\text{conn.}}^d = (2\pi)^3 \delta^D(\vec{k}_o + \vec{k}_p + \vec{k}_q + \vec{k}_r) \times \left\{ \frac{1}{\bar{n}} [B_{(o+p)qr} + \text{perm. (6 terms)}] + \frac{1}{\bar{n}^2} [(P_{o+p+q} + \text{cyc. (4 terms)}) + P_{o+p} + P_{o+q} + P_{o+r}] + \frac{1}{\bar{n}^3} \right\}, \quad (41)$$

$$\langle \delta_1 \dots \delta_6 \rangle_{\text{conn.}}^d = (2\pi)^3 \delta^D(\vec{k}_1 + \dots + \vec{k}_6) \times \left\{ \frac{1}{\bar{n}^3} [B_{12(3\dots+6)} + \text{perm. (15 terms)}] + B_{(1+2)(3+4)(5+6)} + \text{perm. (15 terms.)} + B_{1(2+3)(4+5+6)} + \text{perm. (60 terms)} \right\} + \frac{1}{\bar{n}^4} [P_1 + \dots + P_6 + P_{1+2} + \text{perm. (15 terms)} + P_{1+2+3} + \text{perm. (10 terms)}] + \frac{1}{\bar{n}^5} \}. \quad (42)$$

The correct indices in the permutations and in the cyclical sequences can also be obtained using graph theory (Fry 1984, Bertschinger 1992, Matsubara 1995). The expression for the six-point discrete correlation function is one of the main original results of this work. Its expression is quite complicated, and, it is also important to notice, the discreteness terms do not contribute linearly, but they are multiplied several times by the signal part (B and P) and other noise parts of different order.

3.3 Selection Function

The above analysis is valid for volume-limited samples, where the mean number density is independent of position. In most astronomical catalogues, a selection criterion such as a flux limit introduces a position-dependent mean density, which adds complication to the analysis. However, it turns out that it is very straightforward to include a non-uniform selection function in the generating functional approach, by simply altering the definition of \mathcal{J} . Although we will not apply these results in this paper, we present them for completeness.

Let the mean density be $\bar{n}(\vec{x})$. We follow Feldman, Kaiser & Peacock (1994; hereafter FKP) in defining a fluctuation field

$$F(\vec{x}) \equiv \lambda w(\vec{x}) [n(\vec{x}) - \alpha n_s(\vec{x})], \quad (43)$$

where λ is a normalisation factor, to be determined later, $n(\vec{x})$ is the number density of galaxies, $n_s(\vec{x})$ is the number density of a Poisson-sampled synthetic catalogue with mean density $\bar{n}(\vec{r})/\alpha$, and we consider the limit $\alpha \rightarrow 0$, to avoid shot noise in the synthetic catalogue. $w(\vec{x})$ is an arbitrary weighting function, which may be chosen, as in FKP for example, to minimise the variance in the estimate of the mean power in a shell.

The N -point correlations in Fourier space are most easily calculated by considering the process $f = \lambda w(\vec{x}) n(\vec{x})$ for the galaxy field and similarly for the synthetic catalogue $f_s = -\alpha \lambda w(\vec{x}) n_s(\vec{x})$.

The latter has to be thought as a Poisson sampling of a continuous and uniform underlying process whose density is diluted by a factor α , therefore the generating functional for the process f_s is:

$$\mathcal{Z}_s(\mathcal{J}) = \exp \left\{ \int [\exp(-\alpha i \mathcal{J} \mu w) - 1] \frac{\bar{n}}{\alpha} d^3 x \right\} \quad (44)$$

and \mathcal{J} is given by (31) or (35).

The generating functional for the F process is then given in terms of the generating functional for the galaxies \mathcal{Z}_g by

$$\mathcal{Z}_F(\mathcal{J}) = \mathcal{Z}_g(\mathcal{J}) \mathcal{Z}_s(\mathcal{J}). \quad (45)$$

The subtraction of the synthetic catalogue gives us directly the N -point correlations of the zero-mean field F , by the methods presented in Section 3.2. Equation (45) includes (28) as a particular case when $\alpha \rightarrow 0$.

3.3.1 Power spectrum and Bispectrum

We present here the first two non-trivial terms in the expansion, for illustration, in the case of a volume-limited sample and the general case.

Case (1): Volume-limited catalogue. We choose

$$\lambda = \frac{1}{\bar{n}}, \quad (46)$$

so that $F(\vec{x}) = \delta(\vec{x})$. In this case the transform of $F(\vec{x})$ can be used to get an unbiased estimator of the power spectrum:

$$\langle |F_{\vec{k}}|^2 \rangle = V \left[P_g(k) + \frac{1}{\bar{n}} \right], \quad (47)$$

where V is the volume of the survey. The 3-point function for a closed triangle is

$$\langle F_{\vec{k}_1} F_{\vec{k}_2} F_{\vec{k}_3} \rangle = V \left[B_g(\vec{k}_1, \vec{k}_2, \vec{k}_3) + \frac{1}{\bar{n}} (P_{g1} + P_{g2} + P_{g3}) + \frac{1}{\bar{n}^2} \right]. \quad (48)$$

Comparison with the infinite volume case shows that the Dirac delta function is replaced by $V/(2\pi)^3$. Results for different Fourier transform conventions and power spectrum and bispectrum definitions are given in the Appendix.

Case (2): Varying selection function. We choose

$$\lambda^{-2} = I_{22}, \quad (49)$$

where

$$I_{ij} \equiv \int d^3 \vec{x} w^i(\vec{x}) \bar{n}^j(\vec{x}). \quad (50)$$

Here we find

$$\langle |F_{\vec{k}}|^2 \rangle = P_g(k) + \frac{I_{21}}{I_{22}}, \quad (51)$$

$$\langle F_{\vec{k}_1} F_{\vec{k}_2} F_{\vec{k}_3} \rangle = \frac{I_{33}}{I_{22}^{3/2}} \left[B_g(\vec{k}_1, \vec{k}_2, \vec{k}_3) + \frac{I_{32}}{I_{33}} (P_{g1} + P_{g2} + P_{g3}) + \frac{I_{31}}{I_{33}} \right]. \quad (52)$$

Comparison with the uniform cube shows that to get the N -point functions in the general case the following substitutions may be made:

$$V \rightarrow \frac{I_{NN}}{I_{22}^{N/2}}; \quad \frac{1}{\bar{n}^q} \rightarrow \frac{I_{N(N-q)}}{I_{NN}}. \quad (53)$$

4 THE CHOICE OF TRIANGLES IN EVALUATING THE BISPECTRUM

The methods of Section 3 allow us to calculate the means and covariance matrix for an arbitrary set of triangles, so we may use maximum likelihood to estimate the bias parameters (equation 15). We are left with a question of which triangles to use as our data.

The choice of triangles to analyse is of course very wide. A likelihood analysis could include a very large number of different shapes and sizes, provided that the full covariance matrix is calculated. In practice, CPU and memory considerations force one to consider a subset of triangles, and the analysis is considerably simplified if the covariance matrix is diagonal. This can be achieved by ensuring that any \vec{k} appears in only one triangle (and, since $\delta_{-\vec{k}} = \delta_{\vec{k}}^*$, one must ensure that $-\vec{k}$ doesn't appear elsewhere either). This throws away some of the information, but the number of independent data points is at most 3 times the number one uses with this method, so the information content may not be reduced significantly. The choice of triangle shape is influenced by the behaviour of the bispectrum. As we shall see, most of the signal comes from the largest k -vectors for which second-order perturbation theory holds. We therefore make the vectors as large as possible, and for this paper we choose only equilateral triangles. As discussed in Section 2, a single choice of shape does not allow us to separate b_1 and b_2 . Indeed, in the absence of noise, a single triangle shape determines the combination $b_1/(1+b_2/2Jb_1)$. In this paper, we choose two shapes of triangle, to lift the degeneracy. The first is the equilateral configuration, the second we refer to as 'degenerate', and consists of a repeated vector, and one of twice the amplitude and opposite direction.

In practice the equilateral triangles are obtained as follows: all the k -vectors characterized by a polar angle less or equal to 60° and a longitude angle less or equal to 180° , are considered to be the first vector of a triangle. The second and the third are lying symmetrically in a cone of semi-amplitude 60° centred around $-\vec{k}_1$. Obviously the choice is not unique, and is made at random. The number of actually distinct triangles that one can obtain for a given \vec{k}_1 is limited by the discreteness of the k -space and increases with $|k|$. A similar procedure is followed for the degenerate case, but no wavevectors appear in two triangles (of either shape).

For a discrete grid in a volume-limited cuboidal volume, neighbouring triangles in k -space give uncorrelated estimates of the bispectrum. This feature was checked by investigating the values taken by the off-diagonal terms in the covariance matrix.

We have tested the method with an N -body simulation

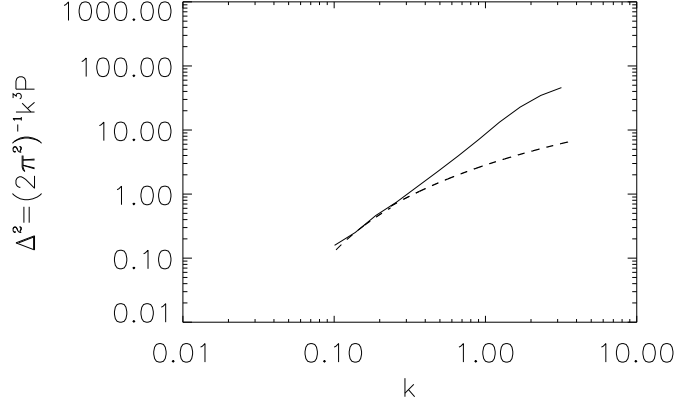


Figure 2. The power spectrum in the N -body simulation (solid), along with the linear power spectrum (dashed).

created with Couchman's (1991) AP^3M code from a Cold Dark Matter (CDM)-like simulation from the Virgo consortium (Jenkins et al. 1996) chosen to match as closely as possible the present-day galaxy power spectrum.

In Fig. 2 we have evidence in the power spectrum for the breakdown of linear perturbation theory at $\Delta_g^2(k) \equiv k^3 P_g(k)/(2\pi^2) \simeq 1$, or at a wavenumber of $k \simeq 0.3$. Fig. 3 and 4 show the bispectrum (for the galaxy field), in the dimensionless form

$$\chi^3 \equiv \left(\frac{2}{\pi^2}\right)^2 B k_1^3 k_2^3 \quad (54)$$

and with this convention

$$\langle \delta^3 \rangle = \int d\cos\theta_1 d\varphi_1 \frac{d\ln k_1}{4\pi} d\cos\theta_2 d\varphi_2 \frac{d\ln k_2}{4\pi} \chi^3(\vec{k}_1, \vec{k}_2). \quad (55)$$

In these figures we see evidence of the breakdown of second-order perturbation at $k \sim 0.6$ for the equilateral triangle, and at a much higher $k \sim 1$ for the degenerate case. The non-linear $\Delta^2(k) \simeq 3$ and 12 respectively (cf Fry, Melott & Shandarin 1995). We use triangles with wavenumbers up to $k = 0.55$ for the equilateral case, and between 0.55 and 1.1 in the degenerate case in the analysis which follows.

In practice, we have used the observed power spectrum (after shot noise subtraction), rather than the linear power spectrum, to calculate the predicted bispectrum ($b_1 = 1$, $b_2 = 0$), shown in Fig. 3 and 4. This includes second-order corrections, but for the leading-order bispectrum term, there is no difference. An alternative would be to linearise the power spectrum, as in Peacock & Dodds (1994), but this requires knowledge of Ω_0 .

4.1 Likelihood analysis

As a first step we analyze the unbiased distribution of mass points, seeking to recover the values $b_1 = 1$ given that $b_2 = 0$.

In the case where the covariance matrix is diagonal the likelihood function is simplified

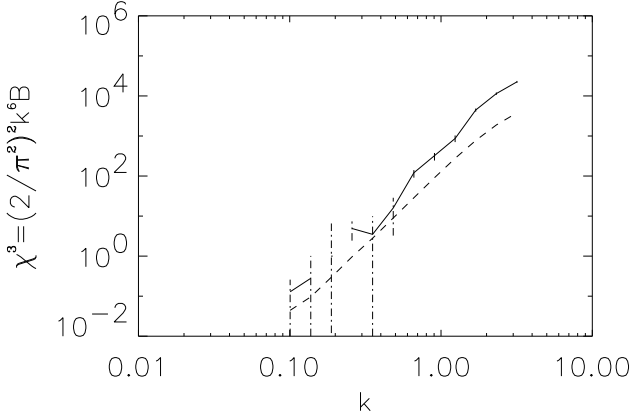


Figure 3. The measured bispectrum from the simulation (solid), with the theoretical prediction from second-order perturbation theory shown dashed. Equilateral triangles are used, and no wavevector appears in more than one triangle. Error bars are errors in the mean for each bin.

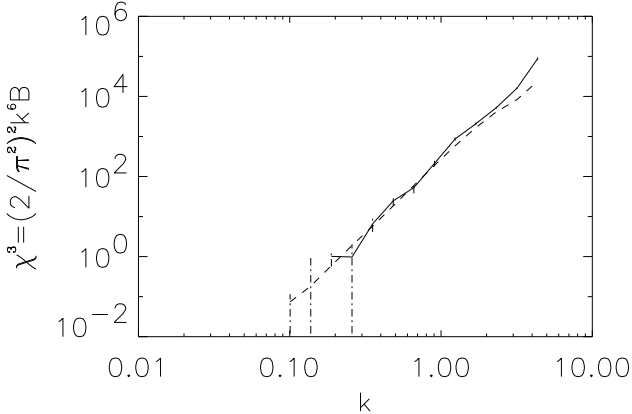


Figure 4. As in Fig. 3, but for ‘degenerate’ triangles k in the abscissa is the smaller wavevector.

$$\mathcal{L}(c_1, c_2) = \frac{1}{(2\pi)^{M/2} \prod_{\alpha} \sigma_{\alpha}} \exp \left\{ -\frac{1}{2} \sum_{\alpha} \frac{(D_{\alpha} - \mu_{\alpha})^2}{\sigma_{\alpha}^2} \right\} \quad (56)$$

and very large numbers of triangles can be used. We have used as many as possible between the largest wavelengths in the cube and the breakdown of second-order perturbation theory (determined above). Fig. 5 shows the likelihood for b_1 , assuming that $b_2 = 0$, from the degenerate and equilateral triangles. The correct value is recovered, within the errors, but the error bar in the equilateral case is uncomfortably large. Rather curiously, the error bar can be reduced

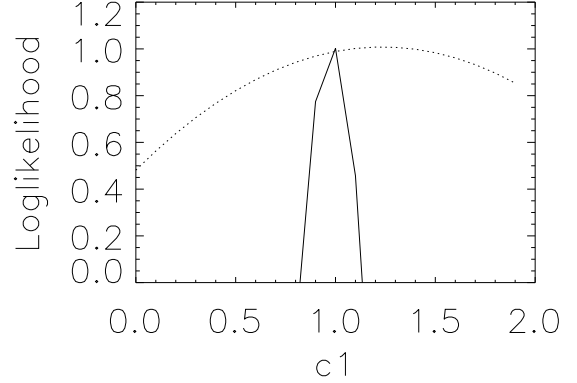


Figure 5. Likelihood of $c_1 = 1/b_1$ where b_1 is the linear bias parameter, for the (unbiased) N -body simulation, for $0.55 < k < 1.1$, using degenerate triangles, and for equilateral triangles (dotted) for $k < 0.55$.

by splitting the volume into sub-samples, as is shown in the next section.

4.2 Expected variance in c_1

We ignore shot noise for simplicity. For equilateral triangles we have:

$$\mu_{\alpha} = \langle D_{\alpha} \rangle = \langle \text{Re}(\delta_{\vec{k}_1} \delta_{\vec{k}_2} \delta_{\vec{k}_3}) \rangle = c_1 \frac{12}{7} P_g^2 \delta^D \equiv c_1 \mu_{\alpha}^{(1)}. \quad (57)$$

The variance in this approximation is

$$\sigma_{\alpha}^2 = \langle D_{\alpha}^2 \rangle - \langle D_{\alpha} \rangle^2 = \frac{1}{2} P_g^3 (\delta^D)^3. \quad (58)$$

The factor of 2 is the same factor as in the transition from complex Z_{α} to real D_{α} in equation (16). Note that of the fifteen signal terms in the covariance matrix $\langle Z_{\alpha} Z_{\beta}^* \rangle$, only one survives. For a discrete transform in a cube of volume V , the Dirac delta function is replaced by $V/(2\pi)^3$, as in (48).

Since σ_{α}^2 is independent of c_1 , the error on c_1 is

$$\sigma_{c_1}^{-2} = - \left. \frac{\partial^2 \ln \mathcal{L}}{\partial c_1^2} \right|_{c_1 = \hat{c}_1} = \sum_{\alpha} \frac{[\mu_{\alpha}^{(1)}]^2}{\sigma_{\alpha}^2}. \quad (59)$$

In practice we are dealing with more than a single mode, and moreover, in k -space the modes form a discrete set, with density of states $g = V/(2\pi)^3$. The number of uncorrelated triangles in a thin shell of width $\delta(\ln k)$ is:

$$\frac{1}{2} 4\pi k^3 \delta(\ln k) g \frac{1}{3}, \quad (60)$$

where the factor $\frac{1}{2}$ arises from the reality of the density fluctuation field and the factor $\frac{1}{3}$ from the requirement of uncorrelated data (no wavevectors in common between any two triangles).

Considering contributions from all the shells, and moving to the continuous limit this becomes:

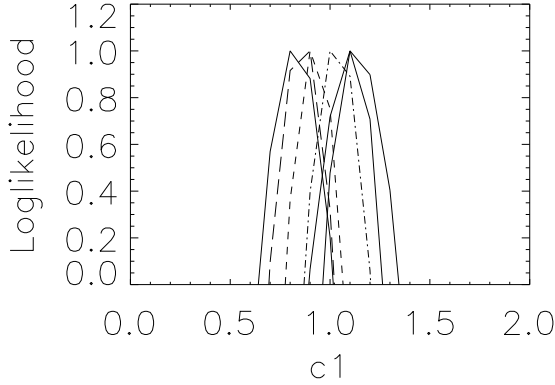


Figure 6. Likelihood of $c_1 = 1/b_1$ for several sub-volumes, each containing 1/8 the volume, for degenerate triangles for the same N -body simulation as Fig. 4.

$$\sigma_{c_1}^{-2} = \frac{V}{12\pi^2} \int_{k_{\min}}^{k_{\max}} d(\ln k) \frac{[\mu(\vec{k})^{(1)}]^2}{\sigma^2(k)} k^3, \quad (61)$$

where k_{\max} is set by the breakdown of perturbation theory, and k_{\min} is set by the size of the sample.

Inserting the appropriate expressions in the previous equation one obtains:

$$\sigma_{c_1}^{-2} = \frac{48}{49} \sigma_0^2(k_{\max}), \quad (62)$$

where

$$\sigma_0^2(k_{\max}) = \frac{1}{2\pi^2} \int_{k_{\min}}^{k_{\max}} d(\ln k) P_g k^3 \quad (63)$$

is the variance in the galaxy field for a top hat filter in k -space truncated at k_{\max} . It is also truncated at the sample size at low- k , which makes the definition slightly non-standard. Hence

$$\sigma_{c_1} \simeq \frac{1.01}{\sigma_0(k_{\max})}, \quad (64)$$

which gives the error of 1.48 seen in Fig. 5, for the cutoff at $k = 0.55$. A curious feature of this analysis is that the error is independent of the size of the survey, motivating the splitting of the volume into independent smaller units. This loses some long-wavelength modes, but these contain little information anyway. Fig. 6 shows the likelihood curves for several sub-volumes, and comparison with Fig. 5 demonstrates that the error is independent of the size of the subvolume. This is somewhat reminiscent of the equally counter-intuitive result that the variance in an estimate of the power spectrum is also independent of the size of the survey, motivating a splitting of the volume as a possible way to increase signal-to-noise in that case (Press et al. 1992).

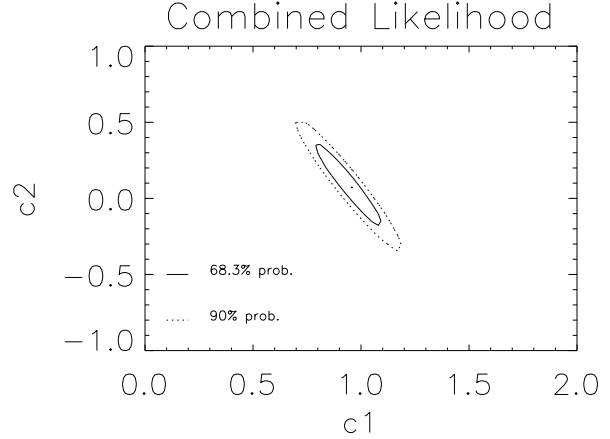


Figure 7. Joint likelihood of $c_1 = 1/b_1$ and $c_2 \equiv b_2/b_1^2$. Contours contain 68.3 and 90 percent of the *a posteriori* probability assuming the likelihood is a bivariate gaussian, and the prior probabilities for c_1 and c_2 are uniform.

4.3 Determining b_1 and b_2

For simplicity, the error analysis of the previous section assumed that the quadratic bias term b_2 is zero. In practice, this may not be true, and we need to estimate both b_1 and b_2 from the data. To lift the degeneracy between b_1 and b_2 , we need to consider at least two triangle configurations. The optimal configurations are not easy to determine, and will certainly depend on the power spectrum, as anything other than the equilateral configuration involves wavenumbers of different magnitude. In addition, each triangle shape leads to approximate determination of a degenerate combination of b_1 and b_2 , so ideally we would like these degenerate lines to cross at large angle. Adding the degenerate triangles to the equilateral configuration is particularly effective, as each degenerate triangle removes only two wavevectors from the available set, and also second-order perturbation theory appears to work well into the nonlinear regime. Fig. 7 shows the joint likelihood for c_1 and c_2 for the limits on k previously stated. The true solution is nicely within the error bars.

5 DISCUSSION

We have presented here the first steps towards the goal of using the bispectrum to measure the linear bias parameter b from large-scale structure data. The aim of this is ultimately to combine measurements of b with estimates of $\beta = \Omega_0^{0.6}/b$ from redshift distortion studies to get an unambiguous estimate of the density parameter Ω_0 . In this paper we have presented a method for calculating the covariance matrix for bispectrum estimates, thus allowing maximum likelihood to be used to estimate b , and tested the methods on N -body simulations. The noise calculation is a general method which will be useful for calculating the properties of any high-order statistics, and is the major new advance of this paper. We

have also shown how the signal-to-noise of the bias estimate may be improved by splitting the volume into subsamples.

It is worth making some remarks about the shape information, as this is crucial in lifting a degeneracy which exists physically between the effect of gravitational evolution and nonlinear bias (in the analysis, this manifests itself as a degeneracy between the linear and quadratic bias terms). In essence, we are exploiting the fact that gravitational instability skews the density field away from its initial Gaussian symmetry. However, this can also be achieved by a nonlinear bias, so we need a further property to distinguish the two. It is the shape information which allows this. Although we work in Fourier space, the argument is most easily stated in real space. The effect of a nonlinear bias, operating on the Gaussian field, is to shift iso-density contours up (or down), but maintaining the shape of the contour. Gravitational evolution, however, will change the shapes, usually leading to flattening of collapsing structures (e.g. Lin, Mestel & Shu 1965). By utilising shape information, we can, in principle, decide to what extent nonlinear biasing and gravitational evolution are responsible for the skewed density field.

A number of unresolved issues remain, and these will be addressed in a subsequent paper. There are two major ones: the practical effects of a varying selection function, and the effect of redshift-space distortions, arising from the fact that the redshift is an imperfect distance indicator because of the contaminating effects of peculiar velocities. This effect can be regarded as being split into two components: a large-scale distortion resulting from coherent inflow into overdense regions, and the ‘Fingers-of-God’ arising from virialised, highly non-linear structures. Since we have argued that it is effective to use subsamples, we would expect to be able to use Kaiser’s (1987) distant-observer approximation, for a deep survey, to model the large-scale distortions (see also Hivon et al. 1995). Of more concern is that most of the signal used to measure the bias parameters comes from the mildly non-linear regime, and it may be that simple models for the Fingers-of-God (such as the incoherent velocity dispersion introduced by Peacock (1992)) may not be adequate for our purposes.

Assuming these problems can be dealt with, the accuracy of the determination of b will be dependent on the number of subvolumes we make, and this is determined by how small the subvolumes may be. From the numerical simulations, we find that the subvolumes degrade significantly the bispectrum estimate if the size of the box is less than about the nonlinear wavelength $2\pi/k_{NL}$, or about $20 h^{-1}$ Mpc for IRAS galaxy data. One would therefore expect rather weak constraints on b from the IRAS PSCz survey, but a much improved error of under 10% from the Sloan digital sky survey or Anglo-Australian 2 degree-field survey. These are rough estimates, based on the shot noise and depth of each survey; it will require more detailed study to see if this accuracy can be achieved or surpassed.

ACKNOWLEDGMENTS

LV acknowledges the support of PPARC and the Dewar & Ritchie fund of the University of Edinburgh. Computations were made using STARLINK facilities. AFH and LV thank the Department of Astronomy in Padova for hospitality. SM

thanks the University of Edinburgh for hospitality. We thank John Peacock, Sergei Shandarin, Francesco Lucchin, Lauro Moscardini, Roman Scoccimarro and Paolo Catelan for useful discussions.

REFERENCES

- Ballinger W.E., Heavens A.F., Taylor A.N., 1995, MNRAS, 276, L59
- Bardeen J.M., Bond J.R., Kaiser N., Szalay A.S., 1986, ApJ, 304, 15 (BBKS)
- Baumgart D.J., Fry J.N., 1991, ApJ, 375, 25
- Bertschinger E., 1992, in Martinez V., Portilla M., Saez D., eds, New insights into the Universe, Proc. Valencia summer school. Springer, Berlin
- Bower R., Coles P., Frenk C.S., White S.D.M., 1993, ApJ, 405, 403
- Catelan P., Coles P., Matarrese S., Moscardini L., 1994, MNRAS, 268, 966
- Catelan P., Lucchin F., Matarrese S., Moscardini L., 1995, MNRAS, 276, 39
- Coles P., 1993, MNRAS 262, 1065
- Couchman H.M.P., 1991, ApJ, 368, 23
- Couchman H.M.P., Carlberg R.G., 1992, ApJ, 389, 453
- Dekel A., Bertschinger E., Yahil A., Strauss M., Davis M., Huchra J., 1993, ApJ, 412, 1
- Feldman H.A., Kaiser N., Peacock J.A., 1994, ApJ, 426, 23
- Fisher K.B., Scharf C.A., Lahav O., 1994, MNRAS, 266, 219
- Frieman J.A., Gaztañaga E., 1994, ApJ, 425, 392
- Fry J.N., 1984, ApJ, 279, 499
- Fry J.N., 1985, ApJ, 289, 10
- Fry J.N., 1994, Phys. Rev. Lett. Vol 73, N 2
- Fry J.N., 1996, ApJ 461, L65
- Fry J.N., Gaztañaga E., 1993, ApJ, 413, 447
- Fry J.N., Melott A.L., Shandarin S.F., 1993, ApJ 412, 504
- Fry J.N., Melott A.L., Shandarin S.F., 1995, MNRAS, 274, 745
- Goroff M.H., Grinstein B., Rey S.-J., Wise M.B., 1986, ApJ, 311, 6
- Hamilton A., 1992, ApJ, 385, L5
- Heavens A.F., Taylor A.N., 1995, MNRAS, 275, 483
- Hivon E., Bouchet F.R., Colombi S., Juszkiewicz R., 1995, A&A, 298, 643
- Jenkins A., Frenk C.S., Pearce F.R., Thomas P.A., Hutchings R., Colberg J.M., White S.D.M., Couchman H.M.P., Peacock J.A., Efstathiou G.P., Nelson A.H., 1996. In ‘Dark and Visible Matter in Galaxies and Cosmological Implications’, Persic, M., Salucci P., ASP conference Series
- Jing Y.P., Börner G., Valdarnini R., 1995, MNRAS, 277, 630
- Kaiser N., 1984, ApJ, 284, L9
- Kaiser N., 1987, MNRAS, 227, 1
- Kendall A., Stuart A., 1977, The Advanced Theory of Statistics, Griffin, London
- Lin C.C., Mestel L., Shu F.H., 1965, ApJ, 142, 1431
- Mann R.G., Peacock J.A., Heavens A.F., 1997, submitted to MNRAS
- Matarrese S., Coles P., Lucchin F., Moscardini L., 1997, MNRAS, 286, 115
- Matarrese S., Lucchin F., Bonometto S.A., 1986, ApJ, 310, L21
- Matsubara T., 1995, ApJS, 101, 1
- Nusser A., Davis M., 1994, ApJ, 421, L1
- Peacock J.A., 1992, in Martinez V., Portilla M., Saez D., eds, New insights into the Universe, Proc. Valencia summer school. Springer, Berlin, p.1
- Peacock J.A., Heavens A.F., 1985, MNRAS, 217, 805
- Peebles P.J.E., 1980, The Large-Scale Structure of the Universe, Princeton University Press, Princeton

Peacock J.A., Dodds, S.J., 1994, MNRAS, 267, 1020
 Press W.H., Teukolsky S.A., Vetterling W.T., Flannery B.P., Numerical Recipes in Fortran, 2nd Edition, C.U.P., Cambridge
 Ramond P., 1989, Field Theory: a Modern Primer, Addison-Wesley, Redwood City
 Rice S.A., Gray P., 1965, The Statistical Mechanics of Simple Liquids. Wiley, New York
 van Kampen N., 1992, Stochastic Processes in Physics and Chemistry. North Holland, Amsterdam
 Williams B.G., Peacock J.A., Heavens A.F., 1991, MNRAS, 252, 43P

APPENDIX A: FOURIER TRANSFORM CONVENTIONS

There are many possibilities for placing of factors of 2π etc. in the definitions of the power spectrum, bispectrum and Fourier transform. These are characterised by the constants A, D and E below. Our choice is $A = 1$, $D = E = (2\pi)^3$, which seems to yield the minimum complexity in the formulae. With the addition of E , this is the same convention as FKP, but differs from Bertschinger (1992), who uses $A = (2\pi)^{-3}$, $D = E = 1$.

$$\begin{aligned} \delta_{\vec{k}} &\equiv A \int d^3x \delta(\vec{x}) \exp(-i\vec{k}\cdot\vec{x}) \\ \langle \delta_{\vec{k}_1} \delta_{\vec{k}_2} \rangle &\equiv DP(k) \delta^D(\vec{k}_1 + \vec{k}_2) \\ \langle \delta_{\vec{k}_1} \delta_{\vec{k}_2} \delta_{\vec{k}_3} \rangle &\equiv EB(\vec{k}_1, \vec{k}_2, \vec{k}_3) \delta^D(\vec{k}_1 + \vec{k}_2 + \vec{k}_3). \end{aligned} \quad (\text{A1})$$

We present below some of the simpler results, including shot noise, with general Fourier conventions for workers whose convention is different from ours. For the case of a varying selection function, the power is

$$\langle |F_{\vec{k}}|^2 \rangle = \lambda^2 \left[\frac{P(k)DI_{22}}{(2\pi)^3} + A^2 I_{21} \right] \quad (\text{A2})$$

and the 3-point function is

$$\begin{aligned} \langle F_{\vec{k}_1} F_{\vec{k}_2} F_{\vec{k}_3} \rangle &= \lambda^3 \left[\frac{EI_{33}}{(2\pi)^3} B(\vec{k}_1, \vec{k}_2, \vec{k}_3) + \right. \\ &\quad \left. \frac{ADI_{32}}{(2\pi)^3} (P_1 + P_2 + P_3) + A^3 I_{31} \right]. \end{aligned} \quad (\text{A3})$$

The conventions may be related to the inverses

$$\begin{aligned} P(k) &= \frac{(2\pi)^3 A^2}{D} \int d^3x \xi^{(2)}(x) \exp(-i\vec{k}\cdot\vec{x}) \\ B(\vec{k}_1, \vec{k}_2, \vec{k}_3) &= \frac{(2\pi)^3 A^3}{E} \int d^3x_{12} d^3x_{23} \\ &\quad \xi^{(3)}(\vec{x}, \vec{x} + \vec{x}_{12}, \vec{x} + \vec{x}_{23}) \exp(-i\vec{k}_2\cdot\vec{x}_{12} - i\vec{k}_3\cdot\vec{x}_{13}) \end{aligned} \quad (\text{A4})$$

(the latter for a closed triangle). The source function for the generating functional in Fourier space is modified in the continuous case from (35) to:

$$\mathcal{J}_{\vec{k}}(\vec{x}) = A \sum_{m=1}^N s_m e^{-i\vec{k}\cdot\vec{x}} \widetilde{W}(\vec{k}_m). \quad (\text{A5})$$